Near-Infrared Photoelectric Properties of Multilayer Bi$_2$O$_2$Se Nanofilms

Hang Yang[1], Wei Chen[2], Xiaoming Zheng[1], Dongsheng Yang[2], Yuze Hu[2], Xiangzhe Zhang[2], Xin Ye[3], Yi Zhang[1], Tian Jiang[2], Gang Peng[1], Xueao Zhang[4*], Renyan Zhang[2*], Chuyun Deng[1*] and Shiqiao Qin[2]

Abstract

The near-infrared (NIR) photoelectric properties of multilayer Bi$_2$O$_2$Se nanofilms were systematically studied in this paper. Multilayer Bi$_2$O$_2$Se nanofilms demonstrate a sensitive photo response to NIR, including a high photoresponsivity (~ 101 A/W), a quick response time (~ 30 ms), a high external quantum efficiency (~ 20,300%), and a high detection rate (1.9×10^{10} Jones). These results show that the device based on multilayer Bi$_2$O$_2$Se nanofilms might have great potentials for future applications in ultrafast, highly sensitive NIR optoelectronic devices.

Keywords: Bi$_2$O$_2$Se, Multilayer, Photodetector, Near-Infrared

Background

Infrared (IR) photodetectors have been widely investigated and studied since their delicate applications in military, commercial, public, and academic domains [1–3]. In the past decade, two-dimensional (2D) materials, for example, graphene, transition metal dichalcogenides (TMDs), and black phosphorus, have grown as promising candidates with great potential for infrared applications [4–9]. Due to the intriguing properties of 2D materials, including the ultrathin thickness, highly mechanical flexibility, suitable and tunable band gap, ultrafast optoelectronic characteristics, and easily tailored van der Waals heterostructures, 2D layered materials have been considered the competitive IR media for next-generation photodetectors [10–12].

Very recently, layered bismuth oxyselenide (Bi$_2$O$_2$Se) was discovered as a promising 2D semiconductor with high electron mobility, ultrafast photoresponse, excellent environmental stability, and easy-accessibility to large production via a facile chemical vapor deposition (CVD) method, making it attractive for electronic and optoelectronic applications [7, 8, 13–15]. Previously, He Jun et al.

[7] and Peng Hailin et al. [8] successively reported that Bi$_2$O$_2$Se owned excellent photoelectric properties to near-infrared (NIR). However, they mainly concerned about thin-layer Bi$_2$O$_2$Se (thickness ~ 7 nm). Prior studies with respect to other 2D materials, such as MoS$_2$ [16] and MoSe$_2$ [17, 18], showed multilayer nanoflakes also owned an extraordinary photoelectric performance compared with monolayer or thin-layer. In fact, multilayer Bi$_2$O$_2$Se may be more attractive than thin-layer Bi$_2$O$_2$Se for FET applications in the thin-film transistor (TFT) configuration [16, 19]. For example, the density of states in multilayer Bi$_2$O$_2$Se is much higher than that in thin-layer Bi$_2$O$_2$Se, which can produce considerably high drive currents in the ballistic limit [13, 14]. In long-channel TFTs, multiple conducting channels can be created by field-effects in multilayer Bi$_2$O$_2$Se, which can boost the current drive of TFTs, similar to silicon-on-insulator MOSFETs [19]. Moreover, multilayer Bi$_2$O$_2$Se offers a wider spectral response than thin-layer Bi$_2$O$_2$Se, due to its narrower bandgap, which can be advantageous in a variety of photodetector applications [20]. Yet, multilayer Bi$_2$O$_2$Se–based photodetectors have not been extensively studied for use in electronics or optoelectronics.

Therefore, the NIR photoelectric properties of multilayer Bi$_2$O$_2$Se (thickness ~ 30 nm) were systematically studied in this paper. Multilayer Bi$_2$O$_2$Se–based photodetector demonstrates an ultra-sensitive photoresponse from 850 to 1550 nm with a good reproducibility at room temperature. Its photoresponsivity reaches 101 A/W at 1000 nm, along

* Correspondence: xazhang@xmu.edu.cn; ryancms@sina.cn; dengchuyun@nudt.edu.cn
[4]College of Physical Science and Technology, Xiamen University, Xiamen 361005, China
[2]College of Advanced Interdisciplinary Studies, National University of Defense Technology, Changsha 410073, China
[1]College of Arts and Science, National University of Defense Technology, Changsha 410073, China
Full list of author information is available at the end of the article

Yang *et al. Nanoscale Research Letters* (2019) 14:371

Page 2 of 6

with a fast rise time and a decay time of 30 ms and 60 ms, respectively. Compared with thin-layer Bi_2O_2Se, multilayer Bi_2O_2Se has higher photoresponsivity and external quantum efficiency, while still keeps a relatively fast response time and a high detection rate. In addition, the photocurrent exhibits a linear dependence on the incident power, offering a good tune ability for multi-purpose applications. These results offer the opportunities for developing the next generation of ultra-sensitive high-performance NIR room-temperature photodetectors.

Methods

Growth and Characterization of Bi_2O_2Se

The Bi_2O_2Se nanofilms were synthesized via a chemical vapor deposition (CVD) method. Bi_2O_3 and Bi_2Se_3 (Alfa Aesar) were located at the center of the horizontal tubular furnace (Lindberg/Blue M), and the mica substrates (Tiancheng Fluorphlogopite Mica Company Ltd., China) were placed downstream as substrates. The furnace was firstly heated to 640 °C with elevation rate of 30 °C min^{-1} and kept for 60 min with an argon gas flow. Finally the furnace was cooled down to room temperature naturally. The synthesized samples were characterized by optic microscope (Olympus BX51), Raman spectrum (WiTec 300R), atomic force microscope (semi-contact mode, NT-MDT company) scanning electron microscope (FEI company). Here, 10-nm

aluminum was firstly thermal evaporated to avoid charge effect of mica substrate before SEM characterization.

Device Fabrication

The photodetector based on multilayer Bi_2O_2Se was fabricated by a standard micro-nano technology. The source and drain contacts were defined by e-beam lithography and followed by depositing a 5 nm Cr/50 nm Au metal stack applying e-beam evaporation. Note that, in order to prevent the charge accumulation on mica substrate during EBL process, conductive polymer photoresist (SX AR-PC-5000) was spin coated on mica prior to the EBL process. Finally, the device was bonded on the chip carrier for further photoelectric measurement.

Performance Measurement

The photocurrent measurements were performed by a homemade xenon lamp (light source: BETICAL HDL-II) photo-detection platform. In the measurement, Keithley 2450 was used to supply the source–drain bias. By switching on/off the light, the drain currents at on/off states were collected. The photoelectric response of the device at different wavelengths (850–1550 nm) could be obtained by substituting different filters.
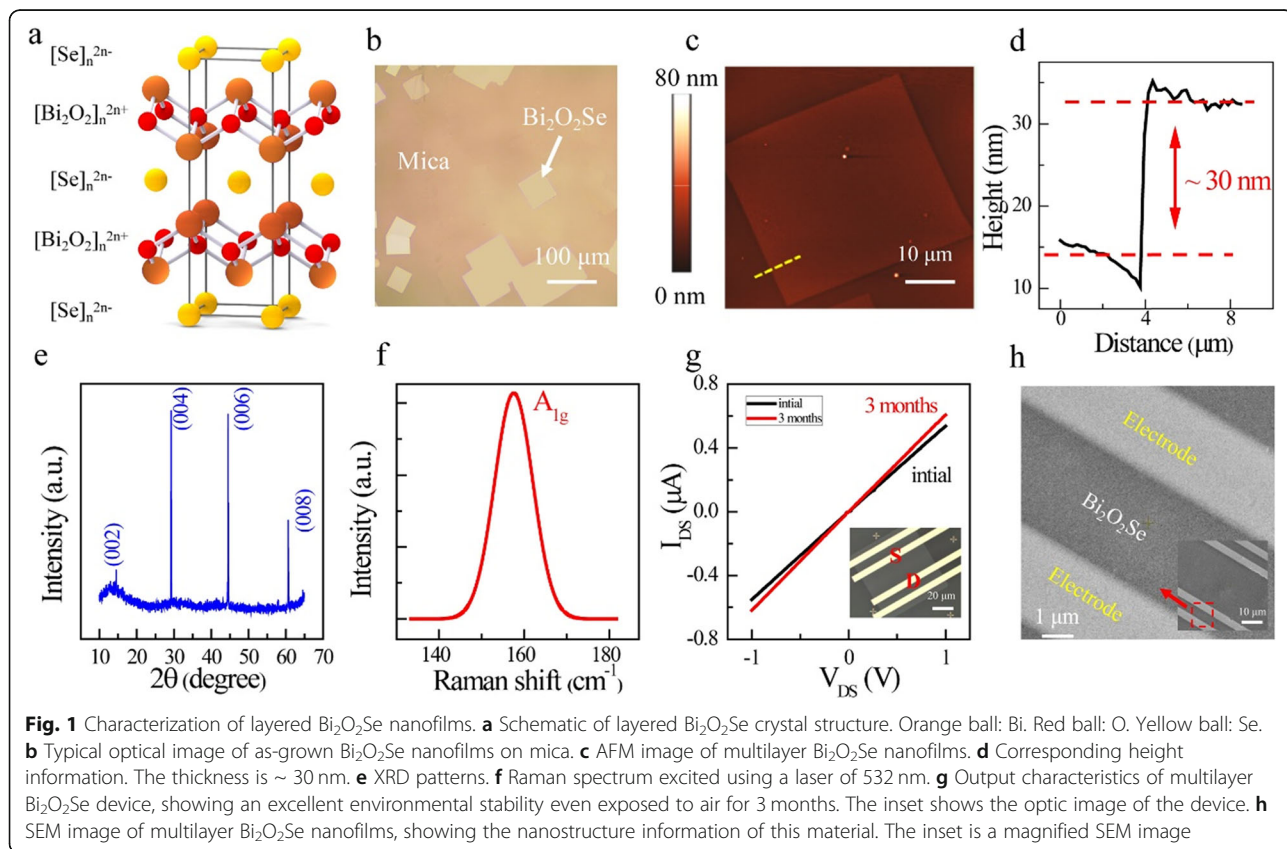

Fig. 1 Characterization of layered Bi_2O_2Se nanofilms. **a** Schematic of layered Bi_2O_2Se crystal structure. Orange ball: Bi. Red ball: O. Yellow ball: Se. **b** Typical optical image of as-grown Bi_2O_2Se nanofilms on mica. **c** AFM image of multilayer Bi_2O_2Se nanofilms. **d** Corresponding height information. The thickness is ~ 30 nm. **e** XRD patterns. **f** Raman spectrum excited using a laser of 532 nm. **g** Output characteristics of multilayer Bi_2O_2Se device, showing an excellent environmental stability even exposed to air for 3 months. The inset shows the optic image of the device. **h** SEM image of multilayer Bi_2O_2Se nanofilms, showing the nanostructure information of this material. The inset is a magnified SEM image
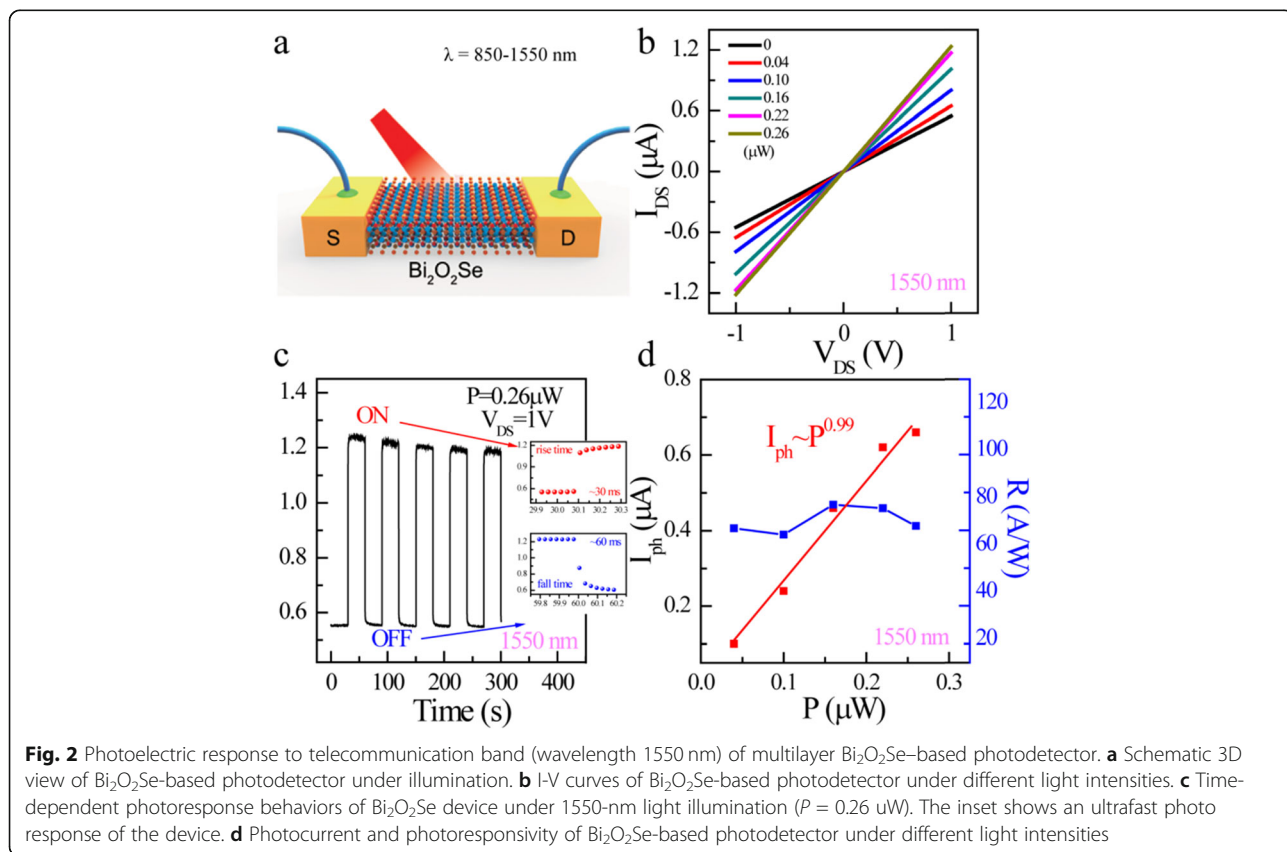
Results and Discussion

As Fig. 1a illustrates, layered Bi_2O_2Se shows a tetragonal structure with I4/mmm space group, and consists of planar covalently bonded oxide layers (Bi_2O_2) sandwiched by Se square arrays with relatively weak electrostatic interactions [21]. This kind of structure is similar to mica. Hence, two-dimensional Bi_2O_2Se nanofilms are all synthesized on the mica substrate by chemical vapor deposition (CVD) method so far [7, 14, 15]. Figure 1b illustrates a large areal optical view of as-grown multilayer Bi_2O_2Se nanofilms on mica. It is clearly seen that the nanofilms are uniform and almost present rectangular shapes. An atomic force microscope (AFM) images of Bi_2O_2Se nanofilms in our experiment are shown in Fig. 1c. According to the theoretical thickness of monolayer (≈ 0.61 nm) [14, 15], 30 nm (Fig. 1d) equals the thickness of around 49 layers. Figure 1e shows the XRD patterns of Bi_2O_2Se nanofilms. Discernable peaks are all attributed to (00l) diffraction planes of Bi_2O_2Se (the crystalline orientation is along *c*-axis), consistent with the previous studies [14]. The characteristic A_{1g} peak of Bi_2O_2Se can be found at ≈ 159.1 cm^{-1} in the Raman spectrum (Fig. 1f), which is in good consistency with the prior reports [22]. Figure 1g shows the typical I-V curve of Bi_2O_2Se device. Excellent linear I-V curve indicates the Ohmic contacts are formed. Besides,

2D Bi_2O_2Se-based photodetector demonstrates an excellent environmental stability, which is a key metric for future practical applications [14, 15]. From Fig. 1h, the measured length and width of the device is 29 μm and 91 μm, respectively.

As Fig. 2a shows, the photoelectric response of multilayer Bi_2O_2Se−based photodetector to NIR was deliberately measured. Here, we mainly discuss the performance of the device in the telecommunication band (1550 nm), which is widely applied in military, commercial, public, and academic domains. It can be seen from Fig. 2b that I_{DS} obviously grows as the light intensity increases. Moreover, the I-V curve of the device under illumination does not demonstrate apparent open circuit voltage and short circuit current. This fact indicates that the Schottky barrier formed between the electrode and the material does not play a pivotal role in the transport characteristic of the device. Therefore, the photoelectric response of the material should mainly come from the photoconductive effect [10].

To evaluate the performance of the photodetectors, photoresponsivity (R), external quantum efficiency (η), and detectivity (D^*) are critical parameters which can be calculated by the following formula [10, 17]:

Fig. 2 Photoelectric response to telecommunication band (wavelength 1550 nm) of multilayer Bi_2O_2Se–based photodetector. **a** Schematic 3D view of Bi_2O_2Se-based photodetector under illumination. **b** I-V curves of Bi_2O_2Se-based photodetector under different light intensities. **c** Time-dependent photoresponse behaviors of Bi_2O_2Se device under 1550-nm light illumination ($P = 0.26$ uW). The inset shows an ultrafast photo response of the device. **d** Photocurrent and photoresponsivity of Bi_2O_2Se-based photodetector under different light intensities

$$R = I_{ph}/PS \tag{1}$$

$$\eta(\lambda) = R_{\lambda}hc/q\lambda \tag{2}$$
$$D^* = I_{ph}/P(2qSI_d)^{1/2} \tag{3}$$

where I_{ph} is photocurrent (the difference of the drain current between illuminated (I_i) and dark (I_d) states), P is the light intensity, S is the effective area, h is the Planck's constant, c is the light velocity, λ is the light wavelength, and q the electronic charge. Here, we assume that the dark current is the major contributor to the shot noise, thus deduce to the equation (3) [7]. This simplification has been used to evaluate the photoresponse of 2D layered materials, like graphene [23] and WSe_2 [24].

As can be seen from Fig. 2c, the device has a very stable and repeatable photoresponse to 1550 nm light after several cycles. Its response time is extremely fast and could reach 30 ms in rise and 60 ms in decay, respectively. This is due to the fact that as-grown ultrathin Bi_2O_2Se nanofilms have no surface trap states and shallow defect energy levels. Finally, as shown in Fig. 2d, I_{ph} increases monotonically with P increasing, following a relationship $I \sim P^{\alpha}$. Here, α is deduced to be 0.99 for Bi_2O_2Se by fitting the experimental data, suggesting that the photocurrent is mainly determined by the amounts of absorbed photon [7]. The photoresponsivity of multilayer Bi_2O_2Se–based photodetectors is around 68 A/W, which exhibits an extremely high performance as a photodetector.

Next, the photoelectric response performance of multilayer Bi_2O_2Se–based photodetector to the NIR wavelengths (850–1550 nm) was systematically studied. According to the calculation by stated formulas (1)–(3), the photoresponsivity, external quantum efficiency and detectivity are demonstrated in Fig. 3. It can be found that the device has a very high photoresponsivity to the NIR band, which reaches 101A/W (900 nm). In addition, multilayer Bi_2O_2Se–based photodetector owns an ultrahigh η, which exceeds 20,000% at 850 nm, indicating its excellent photoelectric conversion capability. Its detection rate can reach 1.9×10^{10} at 900 nm, showing a perfect signal-to-noise ratio as a photodetector. In our measurement, the dark current of the device always maintains at a relatively stable value (0.5 μA). Therefore, the trend of D^* (as a function of incident wavelength) is similar to the trend of R. Obviously, compared with thin-layer Bi_2O_2Se reported by Ref. [7] and Ref. [8], multilayer Bi_2O_2Se has higher photoelectric responsivity and external quantum efficiency (source-drain bias voltage, 1 V, which is the same as Ref. [7] and Ref. [8]), while still keeps a
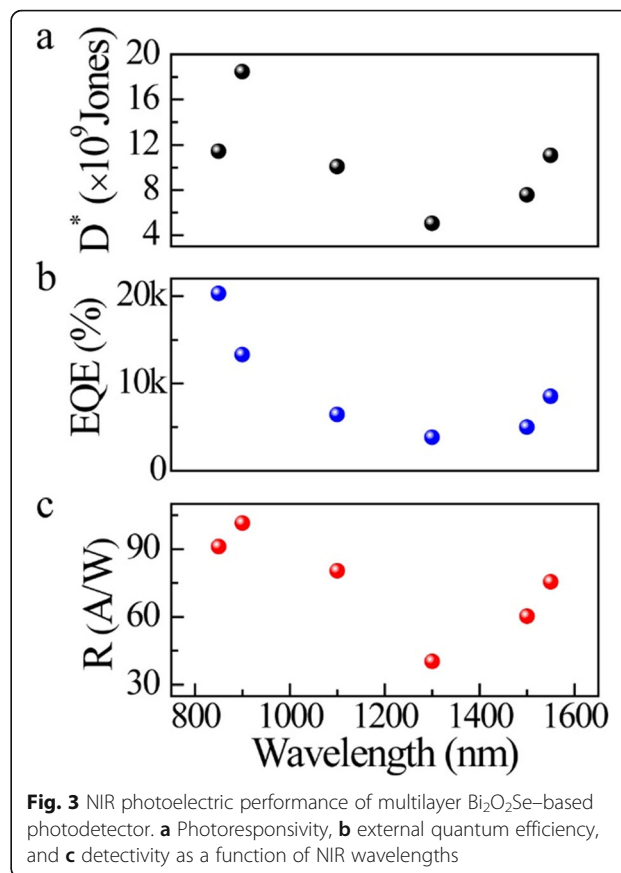

Fig. 3 NIR photoelectric performance of multilayer Bi_2O_2Se–based photodetector. **a** Photoresponsivity, **b** external quantum efficiency, and **c** detectivity as a function of NIR wavelengths

relatively fast response time and high detection rate. Noticeably, Ref. [8] only reported the intrinsic response time (1 ps) of material by pump–probe technique but with no device response time of Bi_2O_2Se photodetectors [8].

In general, 2D layered materials have not yet shown such high sensitivity in NIR detection range. For example, transition metal dichalcogenides (TMDs) usually have too large band gaps to detect IR light [17], while for graphene, it shows high-speed photoresponse but very low intrinsic sensitivity less than tens of mA/W [25]. Although the photoresponsivity can be improved by fabricating atomically heterostructures [26–28], it still does not perform perfectly in the NIR detection. Compared with other 2D materials (Table 1), multilayer Bi_2O_2Se–based photodetector shows a more excellent photoelectric performance, especially a high R and a high η. Noticeably, if the chemical etch was applied to optimize the geometry of multilayer Bi_2O_2Se nanofilms [15], the performance of the device may be further enhanced.

The photo-response physical process of Bi_2O_2Se-based photodetectors can be explained by a simple energy band diagram (Fig. 4a). With no illumination and

Table 1 Comparison of the performance of different room temperature NIR photodetectors. *W* represents response wavelength, *R* represents the photoresponsivity, η represents the external quantum efficiency, D^* represents detectivity, and *t* represents response time

	W (nm)	R (A/W)	η (%)	D^* (Jones)	t	Reference
Multilayer Bi_2O_2Se	850–1550	101	20,300	1.9×10^{10}	< 30 ms	This work
Thin-layer Bi_2O_2Se	808	6.5	999	8.3×10^{11}	2.8 ms	7
Thin-layer Bi_2O_2Se	300–1700	65	——	3.0×10^9	1 ps (intrinsic)	8
Graphene	1550	0.5×10^{-3}	16	——	< 25 ps	25
$MoTe_2$-MoS_2	550–1550	0.046	——	——	25 s	26
GO-GNR	1550	1	80	——	2 s	27
MoS_2/b-P	532–1550	22.3	5000	3.1×10^{11}	70 µs	28

without applying drain bias, the device is in its equilibrium state and with no current flow in the channel. Illuminating the device with NIR light will result in light absorption and excitation of electron-hole pairs, which can be extracted by applying a drain-source bias [29–31]. Since the Schottky barrier in Bi_2O_2Se-metal contact is very low, the photo-generated charge carriers could easily pass the barrier [16–18]. Therefore, multilayer Bi_2O_2Se–based photodetector exhibited an excellent photoelectric performance.

Importantly, the mechanism of enhanced photoelectric performance should be discussed. Theoretically, the optical adsorption of multilayer Bi_2O_2Se is higher than that in thin-layer Bi_2O_2Se, which can induce higher photocurrents I_{ph} [14, 20]. The incident power $P(x)$ as a function of distance x could be expressed as $P(x) = P_{in} \cdot e^{-\alpha \cdot x}$, where α is the absorption coefficient of the Bi_2O_2Se nanofilms at the incident photon energy. The amount of power absorbed by a slab of Bi_2O_2Se with thickness Δx at a distance x from the surface is $dR_a = -(dP/dx) \cdot \Delta x$. Then, the total power absorbed by the Bi_2O_2Se film of thickness d is $R_a = P_{in} \cdot (1 - e^{-\alpha \cdot d})$. For $\alpha \cdot d \ll 1$, the absorbed power can be written as $R_a = P_{in} \cdot \alpha \cdot d$ [16, 19]. Here, the thickness d of in our experiment is 5 times and 3 times of Ref. [7] and Ref. [8], respectively. As a matter of fact, multilayer Bi_2O_2Se nanofilms in our work would have a better R. However, though with the increase of optical adsorption, multilayer Bi_2O_2Se have some drawbacks, such as a higher density of states (DOS), thus causing more mid-gap states compared with monolayer (or thin-layer) [13, 14]. As Fig. 4b shows, when the device turns from "on state" to "off state," the excited electrons in higher bands of multilayer Bi_2O_2Se will firstly transit to the mid-gap states, and then return to ground band [16, 17, 19]. In other words, the carrier lifetime τ will inevitably incline. The same situation will emerge when the device turns from "off state" to "on state." Interestingly, compared with previous work, multilayer Bi_2O_2Se nanofilms still have a fast response time, which is satisfied in many applications [1–3]. This means the existence of mid-gap states may not be detrimental to the dynamic performance of Bi_2O_2Se nanofilms. Last, for greatly enhanced η, two main reasons play pivotal roles. Firstly, the increased layers improve the absorbance of incident photons. In addition, the existence of mid-gap states allows for more transition channels for excited electrons. Thus, η increases significantly [16, 19].
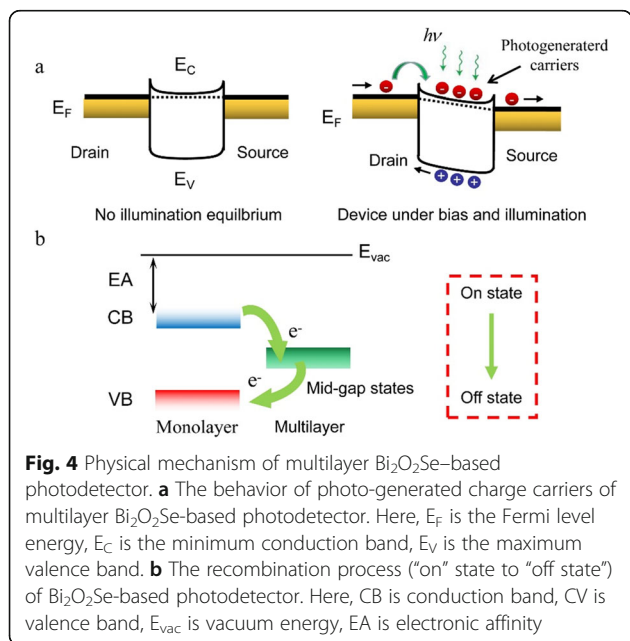

Fig. 4 Physical mechanism of multilayer Bi_2O_2Se–based photodetector. **a** The behavior of photo-generated charge carriers of multilayer Bi_2O_2Se-based photodetector. Here, E_F is the Fermi level energy, E_C is the minimum conduction band, E_V is the maximum valence band. **b** The recombination process ("on" state to "off" state) of Bi_2O_2Se-based photodetector. Here, CB is conduction band, CV is valence band, E_{vac} is vacuum energy, EA is electronic affinity

Conclusions

In summary, we have presented the photoelectric properties of multilayer Bi_2O_2Se (thickness ~ 30 nm)–based photodetector. Multilayer Bi_2O_2Se demonstrates an ultra-sensitive photoresponse from 850 to 1550 nm with good reproducibility at room temperature, including a high photoresponsivity, a quick response time, a high external quantum efficiency, and a high detection rate. Results indicate that multilayer Bi_2O_2Se has a relatively better photoresponse than that of thin-layer.

Yang *et al. Nanoscale Research Letters* (2019) 14:371

Page 6 of 6

Authors' Contributions
HY fabricated the device and wrote the manuscript. XMZ and XZZ carried out the Raman and AFM characterization. HY and YZH conducted the photo-electrical measurement. XY performed the XRD experiment. DSY designed the 3D schematic. WC, RYZ, YZ, GP, and CYD revised the manuscript. XAZ and SQQ supervised the whole work. All authors critically read and approved the final manuscript.

Availability of Data and Materials
All data are fully available without restriction.

Competing Interests
The authors declare that they have no competing interests.

Author details
[1]College of Arts and Science, National University of Defense Technology, Changsha 410073, China. [2]College of Advanced Interdisciplinary Studies, National University of Defense Technology, Changsha 410073, China. [3]Department of Chemistry, National University of Singapore, Singapore 117543, Singapore. [4]College of Physical Science and Technology, Xiamen University, Xiamen 361005, China.

References
1. Lin K-T, Chen H-L, Lai Y-S et al (2014) Silicon-based broadband antenna for high responsivity and polarization-insensitive photodetection at telecommunication wavelengths [J]. Na Commun 5:3288
2. Rogalski A (2011) Recent progress in infrared detector technologies [J]. Infrared Physics Technology 54:136–154
3. Kuo C-H, Wu J-M, Lin S-J et al (2013) High sensitivity of middle-wavelength infrared photodetectors based on an individual InSb nanowire. Nanoscale Res Lett 8:327
4. Chen X, Lu X, Deng B et al (2017) Widely tunable black phosphorus mid-infrared photodetector [J]. Nat Commun 8:1672
5. Jiang T, Zang Y, Sun H et al (2017) Broadband high-responsivity photodetectors based on large-scale topological crystalline insulator SnTe ultrathin film grown by molecular beam epitaxy [J]. Adv Opt Mater 5:1600727
6. Mueller T, Xia F, Avouris P (2010) Graphene photodetectors for high-speed optical communications [J]. Nat Photonics 4:297
7. Li J, Wang Z, Wen Y et al (2018) High-performance near-infrared photodetector based on ultrathin Bi_2O_2Se nanosheets. Adv Funct Mater 28:1706437
8. Yin J, Tan Z, Hong H et al (2018) Ultrafast and highly sensitive infrared photodetectors based on two-dimensional oxyselenide crystals [J]. Na Commun 9:3311
9. Luo S, Wang Y, Tong X et al (2015) Graphene-based optical modulators [J]. Nanoscale Res Lett 10:199
10. Koppens F, Mueller T, Avouris P et al (2014) Photodetectors based on graphene, other two-dimensional materials and hybrid systems [J]. Nat Nanotechnol 9:780
11. Jiang T, Chen R, Zheng X et al (2018) Photo-induced excitonic structure renormalization and broadband absorption in monolayer tungsten disulphide [J]. Opt Express 26:859–869
12. Long M, Wang P, Fang H et al (2019) Progress, challenges, and opportunities for 2D material based photodetectors [J]. Adv Funct Mater 29:1803807
13. Chen C, Wang M, Wu J et al (2018) Electronic structures and unusually robust bandgap in an ultrahigh-mobility layered oxide semiconductor, Bi_2O_2Se [J]. Sci Adv 4:eaat8355
14. Wu J, Yuan H, Meng M et al (2017) High electron mobility and quantum oscillations in non-encapsulated ultrathin semiconducting Bi_2O_2Se [J]. Nat Nanotechnol 12:530
15. Wu J, Liu Y, Tan Z et al (2017) Chemical patterning of high-mobility semiconducting 2D Bi_2O_2Se crystals for integrated optoelectronic devices [J]. Adv Mater 29:1704060
16. Choi W, Cho MY, Konar A et al (2012) High-detectivity multilayer MoS_2 phototransistors with spectral response from ultraviolet to infrared [J]. Adv Mater 24:5832–5836
17. Hang Y, Li Q, Luo W et al (2016) Photo-electrical properties of trilayer $MoSe_2$ nanoflakes [J]. Nano 11:1650082
18. Abderrahmane A, Ko P, Thu T et al (2014) High photosensitivity few-layered $MoSe_2$ back-gated field-effect phototransistors [J]. Nanotechnology 25:365202
19. Kim S, Konar A, Hwang WS et al (2012) High-mobility and low-power thin-film transistors based on multilayer MoS_2 crystals. Nat Commun 3:1011
20. Tian X, Luo H, Wei R et al (2018) An ultrabroadband mid-infrared pulsed optical switch employing solution-processed bismuth oxyselenide. Adv Materi 30:1801021
21. Cheng T, Tan C, Zhang S et al (2018) Raman spectra and strain effects in bismuth oxychalcogenides. J Phys Chem C 122(34):19970–19980
22. Fu Q, Zhu C, Zhao X et al (2018) Ultrasensitive 2D Bi_2O_2Se phototransistors on silicon substrates. Adv Mater 1804945
23. Manga KK, Wang S, Jaiswal M et al (2010) High-gain graphene-titanium oxide photoconductor made from Inkjet Printable Ionic Solution. Adv Mater 22:5265–5270
24. Zhang W, Chiu M-H, Chen C-H et al (2014) Role of metal contacts in high-performance phototransistors based on WSe_2 monolayers [J]. ACS Nano 8:8653–8661
25. Xia F, Mueller T, Lin Y-m et al (2009) Ultrafast graphene photodetector. Nat Nanotechnol 4:839
26. Chen Y, Wang X, Wu G et al (2018) High-performance photovoltaic detector based on $MoTe_2/MoS_2$ van der Waals heterostructure. Small 14:1703293
27. Chitara B, Panchakarla L, Krupanidhi S et al (2011) Infrared photodetectors based on reduced graphene oxide and graphene nanoribbons. Advanced Materials 23:5419–5424
28. Ye L, Li H, Chen Z et al (2016) Near-infrared photodetector based on MoS2/black phosphorus heterojunction. Acs Photonics 3:692–699
29. Zhang X, Zhang R, Zheng X et al (2019) Interlayer difference of bilayer-stacked MoS_2 structure: probing by photoluminescence and Raman spectroscopy. Nanomaterials 9:796
30. Yang H, Qin S, Zheng X et al (2017) An Al_2O_3 gating substrate for the greater performance of field effect transistors based on two-dimensional materials. Nanomaterials 7:286
31. Hao L, Liu Y, Han Z et al (2017) Large lateral photovoltaic effect in MoS_2/GaAs heterojunction. Nanoscale Res Lett 12(1):562

Publisher's Note
Springer Nature remains neutral with regard to jurisdictional claims in published maps and institutional affiliations.